Available online at www.sciencedirect.com
SCIENCE DIRECT®
C. R. Physique 5 (2004) 77–90
COMPTES RENDUS PHYSIQUE

Bose–Einstein condensates: recent advances in collective effects/Avancées récentes sur les effets collectifs dans les condensats de Bose–Einstein

Wave turbulence and Bose–Einstein condensates

Christophe Josserand

Laboratoire de modélisation en mécanique, Université Pierre et Marie Curie and CNRS, case 162, 4, place Jussieu, 75252 Paris cedex 05, France

Presented by Guy Laval

Abstract

The asymptotic behavior of a class of nonlinear Schrödinger equations is studied. Particular cases of 1D weakly focusing and Bose–Einstein condensates are considered. A statistical approach is presented following Jordan and Josserand (Phys. Rev. E 61 (2000) 1527–1539) to describe the stationary probability density of a discretized finite system. Using a maximum entropy argument, the theory predicts that the statistical equilibrium is described by energy equivalued fluctuation modes around the coherent structure minimizing the Hamiltonian of the system. Good quantitative agreement is found with numerical simulations. In particular, the particle number spectral density follows an effective $1/k^2$ law for the asymptotic large time averaged solutions. Transient dynamics from a given initial condition to the statistically steady regime show rapid oscillations of the condensate. ***To cite this article: C. Josserand, C. R. Physique 5 (2004).***

Résumé

Fluctuations turbulentes dans les condensats de Bose–Einstein. Le comportement asymptotique des solutions d'équations différentielles hamiltoniennes est présenté dans le cas général des équations de Schrödinger nonlinéaires. Ce travail reprend une étude précédente s'appuyant sur une description statistique de l'espace des phases de la solution (Phys. Rev. E 61 (2000) 1527–1539). La recherche de la distribution stationnaire à l'équilibre statistique s'effectue pour la dynamique discrète en maximisant l'entropie autour de la solution concentrant toute la masse du système. On trouve alors que la distribution d'équilibre correspond à l'équipartition statistique de l'énergie en excès sur tous les modes accessibles. Les simulations numériques sur un modèles faiblement focalisant et dans le cas particulier d'un modèle 1D de condensat de Bose–Einstein permettent de montrer un bon accord quantitatif avec les prédictions de la théorie. ***Pour citer cet article : C. Josserand, C. R. Physique 5 (2004).***

Keywords: Wave turbulence; Bose-condensate; Statistical equilibrium

Mots-clés : Turbulence d'ondes ; Condensats ; Distribution d'équilibre

1. Introduction

The emergence and persistence of large scale coherent structures in the midst of small scale turbulent fluctuations is a common feature of many turbulent fluids, plasma systems and nonlinear dynamics in general [1–4]. Classical examples include the formation of large vortices in two-dimensional high Reynolds turbulence or the emergence of solitary solutions in nonlinear optics [5,6]. Moreover, and quite surprisingly, such complex phenomena survive even when the dissipationless versions of the dynamics are taken. In these cases as in many classical Hamiltonian systems, the dynamics are formally reversible [7]. Therefore one can question how such apparently irreversible processes can be compatible with these irreversible dynamics? The recent attainment of Bose–Einstein condensates (BEC) [8–10] provides a fascinating new system exhibiting similar behavior. After

E-mail address: josseran@lmm.jussieu.fr (C. Josserand).

1631-0705/$ – see front matter
doi:10.1016/j.crhy.2004.01.004

being attained, the condensate can indeed be viewed as a large coherent structure, persisting in the atomic trap and surrounded by fluctuations. When thermal fluctuations are neglected, BEC can be modelled by the usual semi-classical Gross–Pitaevskii equation. It is strictly valid only at $T = 0$ and is also Hamiltonian dynamics. Moreover, note that for all these examples the dynamics resume in partial differential equations describing the evolution of one or few classical fields (velocity for turbulent flows or wave function for BEC for instance).

The interplay between the fluctuations and the coherent structures in these systems is of crucial interest to our understanding of nonlinear dynamics. Important questions are related to the asymptotic behavior of the dynamics and to their possible statistical description. In particular, the expected thermal equilibrium would in fact lead to the well-known Rayleigh–Jeans divergences for a classical field. The aim of this article is precisely to investigate how this black body-like catastrophe manifests in the a priori smooth dynamics, driven by the partial differential equations (PDE) considered here. For simplified reversible models, it is believed and borne out by numerical simulations that the coherent structures may act as statistical attractors to which the whole system relaxes. Following weak turbulence theory, in continuum systems, the fluctuations were shown to decrease without bound in addition to cascading to smaller and smaller scales. The explanations proposed for this cascade-like process invoke in fact thermodynamical considerations [11,12]. In collaboration with R. Jordan, we have recently focused on such scenario for the class of nonintegrable nonlinear Schrödinger (NLS) equations [13,14]. Following [15] we seek the probability density of a solution for a finite number n of modes version of the NLS equations. Usual thermodynamical arguments, where the probability density corresponds to the standard Maxwell–Boltzmann distribution, fail, and one has to consider that a coherent structure emerges from the solution of the PDE. Indeed, from numerical simulations we assume the presence of a non-zero mean field which contains most of the conserved particle number (L^2-norm squared). Such specific treatment of a particular part of the solution is therefore very close to the statistical theory of the Bose–Einstein transition! The stationary probability distribution is obtained *via* the maximization of the entropy of this finite statistical system. It describes an ensemble where the mean-field corresponds to a large-scale coherent solitary wave, which minimizes the Hamiltonian given the particle number, coupled with small-scale random fluctuations, or radiation. The fluctuations equally share the difference of the conserved value of the Hamiltonian and the Hamiltonian of the coherent state. The effective temperature of this thermal-like system is inversely proportional to n, the number of modes, and goes therefore to zero in the continuum limit. Thus the discretization level n of the dynamics triggers an effective energy cut-off which avoids the Rayleigh–Jeans divergencies. This statistical theory found very good qualitative and quantitative agreement with numerical simulations done for a weakly focusing NLS equation. Statistical ensemble can be retrieved by time and ensemble averaging of large time numerical solutions starting from random initial conditions. At large enough time, the dynamics of the solutions present statistical stationary properties in full agreement with the statistical theory. The road to this statistically stationary state is also investigated and allows a consistent scenario for the dynamics in the continuum limit $n \to \infty$.

In this article, we discuss how these results apply to the case of BEC dynamics. The Gross–Pitaevskii equation in harmonic trap used to model the condensate evolution is in fact a particular case of NLS system so that the introduced description is valid. Before that, the general theory for the NLS equation in one spatial dimension with a finite number of modes will be presented in detail.

2. Self-organization in NLS-systems

In this section I briefly introduce the results obtained for the NLS-equations. Most of the conclusions and the figures are presented for a specific 1-D focusing NLS equation but the results apply to the whole class of these models. The presentation here will follow [13] and the reader will find more details and references there.

2.1. Generalities

We consider the general dimensionless NLS equation:

$$\mathrm{i}\partial_t \psi + \Delta\psi + f\left(|\psi|^2\right)\psi = 0, \tag{1}$$

where $\psi(\mathbf{r}, t)$ is a complex field and Δ is the Laplacian operator. The function $f(|\psi|^2)$ stands for nonlinear interaction and external potential. Among other phenomena, it is used to model gravity waves on deep water [16], Langmuir waves in plasmas [6], pulse propagation along optical fibers [3], superfluid dynamics [17] and Bose–Einstein condensates [18]. In this latter case, the interaction function $f(|\psi|^2)$ depends also on the position $\mathbf{r}$ to describe the atomic trap in which Bose–Einstein condensates are achieved. When $f(|\psi|^2) = \pm|\psi|^2$ and Eq. (1) is posed on the whole real line or on a bounded interval with periodic boundary conditions, the equation is completely integrable [20]. In any other configuration it is nonintegrable.

The Hamiltonian equation associated to (1) is: $\mathrm{i}\partial_t\psi = \delta H/\delta\psi^*$, where ψ^* is the complex conjugate of the field ψ, and H is the Hamiltonian:

$$H(\psi) = \int \left(|\nabla\psi|^2 - F\left(|\psi|^2\right)\right) \mathrm{d}\mathbf{r}. \tag{2}$$

Here, in addition to the kinetic term $|\nabla\psi|^2$, the *potential* F is defined via the relation $F(a) = \int_0^a f(y)\,\mathrm{d}y$. The dynamics (1) conserve, in addition to the Hamiltonian, the particle number (also called the mass)

$$N(\psi) = \int |\psi|^2 \,\mathrm{d}\mathbf{r}. \tag{3}$$

Without loss of generality we hereafter restrict the statistical analysis and the numerics to nonintegrable models in one spatial dimension. Eq. (1) exhibits solitary wave solutions $\psi = \phi(x,t)\,\mathrm{e}^{\mathrm{i}\lambda^2 t}$ which satisfy

$$\phi_{xx} + f\left(|\phi|^2\right)\phi - \lambda^2\phi = 0. \tag{4}$$

It is worthwhile to notice that the solution of Eq. (4) minimizes the Hamiltonian (2) for a given particle number. We will denote $H^*(N)$ the value of the energy of this solution. These localized structures are found to play an important role in the time evolution of Eq. (1). Fig. 1 indeed, shows snapshot of the dynamics for the weakly focusing nonlinearity $f(|\psi|^2) = |\psi|$. Starting with a slightly perturbed homogenous solution, a collection of solitary peaks emerge from this linearly unstable state. These solitary waves rapidly coalesce into a single coherent structure surrounded by small amplitude fluctuations. A slow, quasistatic dynamics follows where the fluctuations are seen to decrease in wavelength and in amplitude. The solitary structure gathers almost all the mass of the system while the energy reaches smaller scales. In other words, the dynamics presents the *condensation* of the mass into a coherent structure while the energy is distributed in the system.

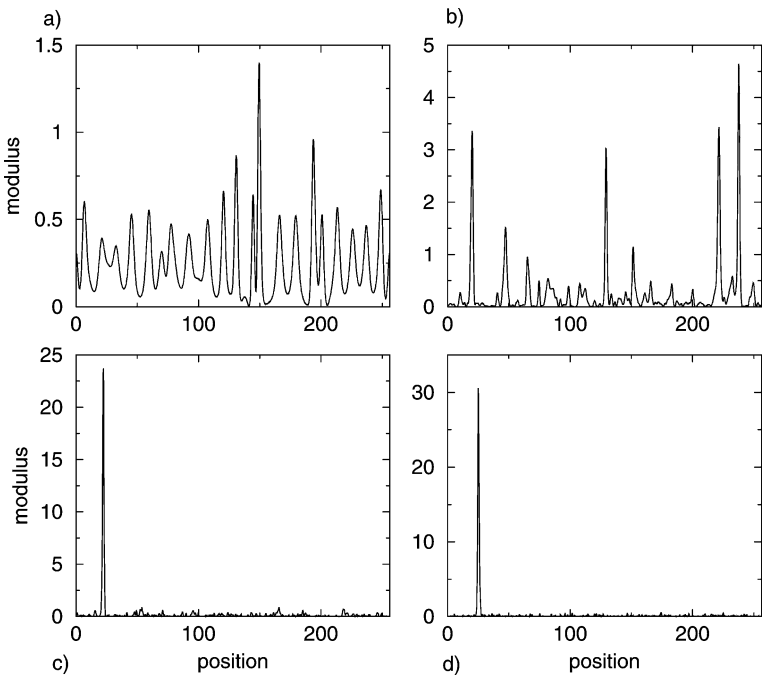

Fig. 1. Profile of the modulus $|\psi|^2$ at four different times for the system (1) with nonlinearity $f(|\psi|^2) = |\psi|$ and periodic boundary conditions on the interval $[0, 256]$. The initial condition is $\psi(x, t=0) = A$, with $A = 0.5$, plus a small random perturbation. The numerical scheme used to approximate the solution is the split-step Fourier method. The grid size is $\mathrm{d}x = 0.125$, and the number of modes is $n = 2048$. (a) $t = 50$ unit time: due to the modulational instability, an array of soliton-like structures separated by the typical distance $l_i = 2\pi/\sqrt{A/2} = 4\pi$ is created; (b) $t = 1050$ unit time: the solitons interact and coalesce, giving rise to a smaller number of solitons of larger amplitude; (c) $t = 15\,050$: The coarsening process has ended. One large soliton remains in a background of small-amplitude radiation. Notice that for $t = 55\,050$ unit time (d), the amplitude of the fluctuations has diminished while the amplitude of the soliton has increased.

2.2. Statistical model

To explain these numerical observations, we construct a consistent mean-field statistical theory based on [15]. It seeks to describe the solution as a mean field which contains most of the particle number of the system while the amount of energy not accounted by this solution is dispersed towards small scales. The theory is in fact presented for finite dimensional approximation of the NLS equation, using also the Dirichlet boundary conditions on the interval $[0, L]$. Other boundary conditions, such as the periodic ones used in the simulations can easily be considered without any change in the conclusions.

Let $e_j(x) = \sqrt{2/L}\sin(k_j x)$ with $k_j = \pi j/L$, and for any function $g(x)$ on $\Omega = [0, L]$ denote by $g_j = \int_\Omega g(x)e_j(x)\,\mathrm{d}x$ its jth Fourier coefficient with respect to the orthonormal basis e_j, $j = 1, 2, \ldots$. We consider now a truncated version of the NLS equations to the n first Dirichlet modes. We write $\psi^{(n)} = u^{(n)} + \mathrm{i}v^{(n)}$, where $u^{(n)}$ and $v^{(n)}$ are two real functions whose Fourier coefficients satisfy the coupled system of ordinary differential equations

$$\dot{u}_j - k_j^2 v_j + \left(f\left(\left(u^{(n)}\right)^2 + \left(v^{(n)}\right)^2\right)v^{(n)}\right)_j = 0, \tag{5}$$

$$\dot{v}_j + k_j^2 u_j - \left(f\left(\left(u^{(n)}\right)^2 + \left(v^{(n)}\right)^2\right)u^{(n)}\right)_j = 0. \tag{6}$$

It corresponds for $\psi^{(n)}$ to:

$$\mathrm{i}\psi_t^{(n)} + \psi_{xx}^{(n)} + P^n\left(f\left(\left|\psi^{(n)}\right|^2\right)\psi^{(n)}\right) = 0,$$

where P^n is the projection onto the span of the eigenfunctions $e_1, \ldots, e_n$. This equation is a natural spectral approximation of the NLS equation (1), and it may be shown that its solutions converge as $n \to \infty$ to solutions of (1) [19,21].

For given n, the system of Eqs. (6) defines a dynamics on the $2n$-dimensional phase space $\mathbf{R}^{2n}$. This finite-dimensional dynamical system is a Hamiltonian system, with conjugate variables u_j and v_j, and with Hamiltonian

$$H_n = K_n + \Theta_n, \tag{7}$$

where

$$K_n = \frac{1}{2}\int \left(\left(u_x^{(n)}\right)^2 + \left(v_x^{(n)}\right)^2\right)\mathrm{d}x = \frac{1}{2}\sum_{j=1}^{n} k_j^2\left(u_j^2 + v_j^2\right), \tag{8}$$

is the kinetic energy, and

$$\Theta_n = -\frac{1}{2}\int F\left(\left(u^{(n)}\right)^2 + \left(v^{(n)}\right)^2\right)\mathrm{d}x, \tag{9}$$

is the potential energy. The Hamiltonian H_n is, of course, an invariant of the dynamics. The truncated version of the particle number, up to a multiplicative factor in the definition

$$N_n = \frac{1}{2}\int \left(\left(u^{(n)}\right)^2 + \left(v^{(n)}\right)^2\right)\mathrm{d}x = \frac{1}{2}\sum_{j=1}^{n}\left(u_j^2 + v_j^2\right), \tag{10}$$

is also conserved by the dynamics (6).

We argue that we can build a statistical treatment of the system using the usual assumption that the dynamics is ergodic and noting also that system (6) satisfies the Liouville property (the measure $\prod_{j=1}^{n}\mathrm{d}u_j\,\mathrm{d}v_j$ is invariant) [22].

We thus replace the time dependant dynamics by a statistical (time independent) description of the solution at any time. We introduce a probability density $\rho^{(n)}(u_1, \ldots, u_n, v_1 \ldots, v_n)$ on the $2n$-dimensional phase space and we seek the density function $\rho^{(n)}$ which maximizes the Gibbs–Boltzmann entropy functional:

$$S(\rho) = -\int_{\mathbf{R}^{2n}} \rho\log\rho\prod_{j=1}^{n}\mathrm{d}u_j\,\mathrm{d}v_j. \tag{11}$$

We easily obtain the usual canonical ensemble solution:

$$\rho \propto \exp(-\beta H_n - \mu N_n),$$

subject to the mean constraints $\langle H_n\rangle = H^0$ and $\langle N_n\rangle = N^0$. H^0 and N^0 are the given values of the Hamiltonian and the particle number, respectively, and β and μ are the Lagrange multipliers associated to these constraints. Such a density is actually ill-defined since it is not normalizable (i.e., $\int_{\mathbf{R}^{2n}}\exp[-\beta H_n - \mu N_n]\prod_{j=1}^{n}\mathrm{d}u_j\,\mathrm{d}v_j$ diverges) for the focusing nonlinearities we

discuss here [15,24]. Moreover, this distribution does not take into account the numerical observed fact that an important part of the phase space consists of configurations where most of the mass is concentrated in the solitary wave solution.

Inspired by these remarks, we have built an adapted statistical description of the dynamics. We decompose the fields u_n and v_n into two contributions: the means denoted $\langle u_j\rangle$ and $\langle v_j\rangle$ and the fluctuations $(\delta u^{(n)}, \delta v^{(n)}) \equiv (u^{(n)} - \langle u^{(n)}\rangle, v^{(n)} - \langle v^{(n)}\rangle)$. This decomposition will be clarified by the yet to be determined ensemble $\rho^{(n)}$. We now impose that in the long-time NLS dynamics (6) and for the continuum limit $n \to \infty$, the amplitude of the fluctuations vanishes. Consequently, the number of particles in this limit is almost determined by the mean field. The vanishing fluctuations hypothesis is written:

$$\int_\Omega \left[\left\langle \left(\delta u^{(n)}\right)^2\right\rangle + \left\langle \left(\delta v^{(n)}\right)^2\right\rangle\right] \mathrm{d}x \equiv \sum_{j=1}^{n} \left[\left\langle (\delta u_j)^2\right\rangle + \left\langle (\delta v_j)^2\right\rangle\right] \to 0, \quad \text{as } n \to \infty. \tag{12}$$

Using this assumption, it follows that for n large enough, the total number of particles is well approximated by the mean contribution. Similarly, one can show that the potential energy is almost entirely determined by the potential of the mean. However, although the fluctuations do not contribute much to the particle number and the potential energy, they may have a significant kinetic energy. Indeed, this contribution $(1/2)\sum_{j=1}^{n} k_j^2[\langle(\delta u_j)^2\rangle + \langle(\delta v_j)^2\rangle]$, need not tend to 0 as $n \to \infty$, even if (12) holds. Actually, it must in general not tend to 0 since the total energy of the system is conserved.

From these remarks, we can impose the following mean-field constraints on ρ:

$$\widetilde{N}_n(\rho) \equiv \frac{1}{2}\sum_{j=1}^{n}\left(\langle u_j\rangle^2 + \langle v_j\rangle^2\right) = N^0, \tag{13}$$

$$\widetilde{H}_n(\rho) \equiv \frac{1}{2}\sum_{j=1}^{n} k_j^2\left(\left\langle u_j^2\right\rangle + \left\langle v_j^2\right\rangle\right) - \frac{1}{2}\int_\Omega F\left(\left\langle u^{(n)}\right\rangle^2 + \left\langle v^{(n)}\right\rangle^2\right) \mathrm{d}x = H^0. \tag{14}$$

Here N^0 and H^0 are precisely the conserved values of the particle number and the energy, as determined from initial conditions.

The solutions $\rho^{(n)}$ of the statistical equilibrium states with the particle number constraint (13) are calculated now, invoking again a maximum entropy principle. Notice that, similar to its above use, this principle has no reason to hold in such Hamiltonian and reversible systems. However, it allows a consistent calculation of the density following an ergodic assumption [22]. It somehow corresponds to the determination of the density distribution around the most probable state (see also for a further discussion the recent work [23]).

The solutions $\rho^{(n)}$ are therefore calculated through usual techniques: two Lagrange multipliers are used to enforce the mass and the energy constraints. Considering independent statistical variables, the factorization of the maximum entropy distribution is straightforward:

$$\rho^{(n)}(u_1, \ldots, u_n, v_1, \ldots, v_n) = \prod_{j=1}^{n} \rho_j(u_j, v_j), \tag{15}$$

where, for $j = 1, \ldots, n$,

$$\rho_j(u_j, v_j) = \frac{\beta k_j^2}{2\pi} \exp\left\{-\frac{\beta k_j^2}{2}\left(\left(u_j - \langle u_j\rangle\right)^2 + \left(v_j - \langle v_j\rangle\right)^2\right)\right\}. \tag{16}$$

In addition, we find that the complex field $\langle\psi^{(n)}\rangle = \langle u^{(n)}\rangle + i\langle v^{(n)}\rangle$ is a solution of (setting $\lambda = \mu/\beta$)

$$\left\langle\psi^{(n)}\right\rangle_{xx} + P^n\left(f\left(\left|\left\langle\psi^{(n)}\right\rangle\right|^2\right)\left\langle\psi^{(n)}\right\rangle\right) - \lambda\left\langle\psi^{(n)}\right\rangle = 0, \tag{17}$$

which is clearly the spectral truncation of the eigenvalue equation (4) for the continuous NLS system (1). It follows, therefore, that the mean-field predicted by our theory corresponds to a solitary wave solution of the NLS equation. On the other hand, the fluctuations δu_j and δv_j are independent Gaussian variables with identical variance $1/\beta k_j^2$.

The energy constraint (13) imposes:

$$H^0 = \frac{n}{\beta} + H_n\left(\left\langle u^{(n)}\right\rangle, \left\langle v^{(n)}\right\rangle\right), \tag{18}$$

where the term $\frac{n}{\beta}$ reflects the equipartition of energy among the $2n$ independent fluctuating modes. The calculation of the total entropy is straightforward:

$$S\left(\rho^{(n)}\right) = C(n) + n\log\left(\frac{L^2[H^0 - H_n(\langle u^{(n)}\rangle, \langle v^{(n)}\rangle)]}{n}\right), \tag{19}$$

where $C(n) = n - \sum_{j=1}^{n} \log(j^2\pi/2)$ depends only on the number of Fourier modes n. Thus, the key results follow the maximization of the entropy: firstly the mean-field pair $(\langle u^{(n)}\rangle, \langle v^{(n)}\rangle)$ has in fact to realize the minimum possible value of H_n over all fields $(u^{(n)}, v^{(n)})$ that satisfy the constraint $N_n(u^{(n)}, v^{(n)}) = N^0$. Moreover, the excess energy not present in the mean field is equally distributed among the fluctuating modes, with the inverse temperature:

$$\beta = \frac{n}{H^0 - H_n^*}, \tag{20}$$

where H_n^* is precisely this minimum value of H_n allowed by the particle number constraint $N_n = N^0$. We obtain also that the inverse temperature scales linearly with the number of modes in the continuum limit.

The vanishing of fluctuations hypothesis is also verified if one computes the contribution of the fluctuations to the number of particles. It can be written:

$$\frac{1}{2}\sum_{j=1}^{n}\left[\left\langle(\delta u_j)^2\right\rangle + \left\langle(\delta v_j)^2\right\rangle\right] = \frac{H^0 - H_n^*}{n}\sum_{j=1}^{n}\frac{1}{k_j^2} = \mathrm{O}\left(\frac{1}{n}\right), \quad \text{as } n \to \infty. \tag{21}$$

The limitation of our statistical description follows directly from Eq. (21). Indeed, for a fixed number of modes n, the coherent structure can only emerge if $N \gg (H^0 - H_n^*)/n$. If this criterion is not satisfied, the condensation of the solution into the coherent structure can even be broken. In fact, it is still under debate whether such a coherent structure can emerge in the continuum limit when starting with a highly fluctuating state concentrated at relatively small wavelengths [26]. In this approach the fluctuation modes have been choosen as the $e_j(x)$ Fourier functions. This assumption is in fact a direct consequence of the factorization of the entropy, considering independent Fourier coefficients. Such an hypothesis is correct for defocusing homogenous NLS equation but is, in general, only valid for a large wave number k_j. Indeed, it is well known by linearizing Eq. (1) around a given state that the perturbation modes have to be found through the so called Bogoliubov theory. Although the full determination of the Bogoliubov modes is needed to improve the statistics, we note that plane waves are a good approximation of the fluctuation modes for large enough k_j so that our theory is always relevant to describe the statistics of the small wavelength perturbations.

Finally, regardless of these restrictions, our statistical equilibrium approach gives the following prediction for the particle number spectral density:

$$\left\langle|\psi_j|^2\right\rangle = \left|\langle\psi_j\rangle\right|^2 + \frac{H^0 - H_n^*}{nk_j^2}, \tag{22}$$

where we have used the identity $\psi_j = u_j + \mathrm{i}v_j$.

2.3. Numerical results

In [13], we discuss how numerical simulations compare with these statistical predictions. Starting from any set of initial condition, one expects, following ergodic theory, that large time and large ensemble (over different initial conditions) averages will reproduce the statistical description of the system. Alternatively, one can choose to measure 'quasi-static' averaged quantities by measuring only few time unit averages and (if possible) large ensemble average. Such quasi-static description would converge to the sought after statistical regime for large enough integration time of the dynamics where the transitory effects due to the initial conditions can be ignored. We address here the weakly focusing nonlinearity $f(|\psi|^2) = |\psi|$ already used for Fig. 1. The transient dynamics can be estimated by plotting the two contributions to the conserved total energy. Fig. 2 shows over a large period the evolution of the kinetic and the potential energy, averaged over 16 slightly noisy homogenous states. Fast but small oscillations of the energies around a smooth evolution account for the rapid fluctuation modes. The kinetic (potential) energy is then found to increase (decrease) as time goes on, indicating the transfer of energy towards smaller scale. Moreover, after a short transient (until $t = 50\,000$ time units) corresponding to the formation of peaks and to their coalescence into one single structure, a slow quasistatic regime is observed as described in Fig. 1. This slow evolution witnesses the convergence of the coherent structure to the Hamiltonian minimizer. The straight line below the potential energy indicates the potential energy of the minimizer for the total particle number N_0. The potential energy approaches a constant value close to this bound, the difference being due to the finite particle number which still remains in the fluctuations. This quasistatic dynamics seems in fact to saturate for this n-modes calculations at large time ($t \geqslant 900\,000$). Indeed, such convergence is observed on the mean particle number spectra averaged over few time units and 16 initial conditions, which shows stationary properties thereafter.

Fig. 3 shows this particle number spectral density. The spectral density of the solitary solution which contains the total initial particle number is drawn (smooth line) for comparison. The equipartition for large wavenumber deduced from the theory is also marked, corresponding to a straight line in the log–log plot. Very good quantitative agreements are found between the theoretical predictions and the numerics, for the coherent structure at large scale as well as for the $1/k^2$ spectrum for small scale.

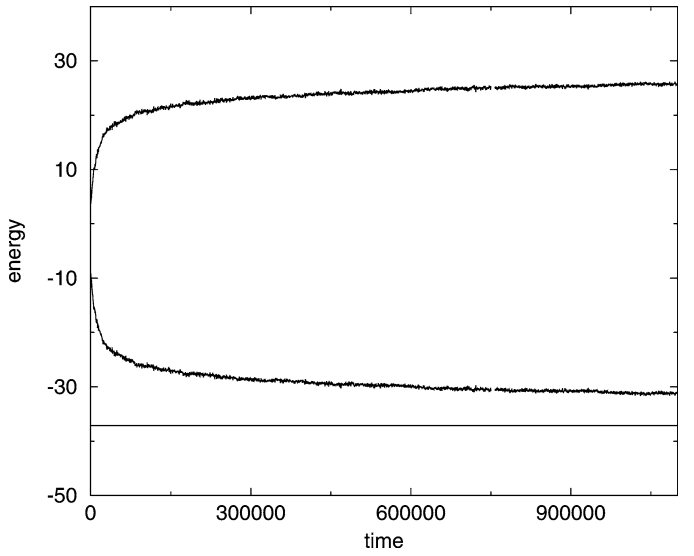

Fig. 2. Kinetic (top curve) and potential (bottom curve) energies as function of time for the weakly focusing NLS. The straight line below the potential energy corresponds to the potential energy of the minimizer of the Hamiltonian for the particle number. The calculations are made with $n = 512$ discretization points and ensemble averaged is performed over 16 different initial configurations.

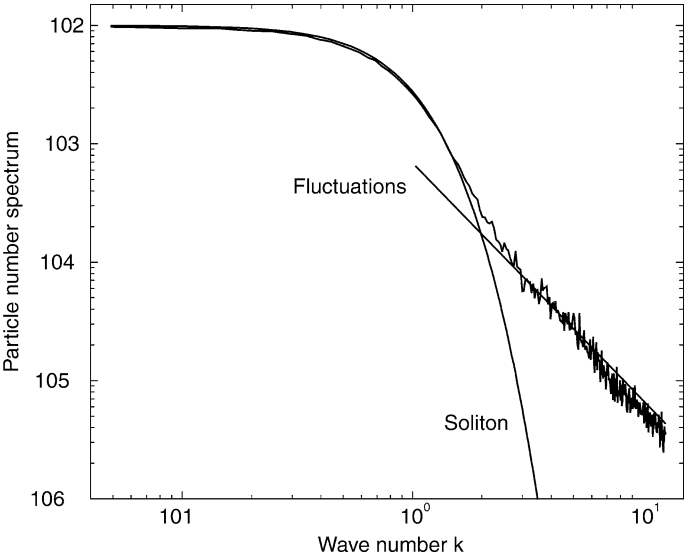

Fig. 3. Particle number spectral density $|\psi_k|^2$ as a function of k for $t = 1.1 \times 10^6$ unit time (upper curve). The lower curve (smooth one) is the particle number spectral density for the solitary wave that contains all the particles of the system. The straight line drawn for large k corresponds to the statistical prediction (22) for the spectral density for large wavenumbers. The numerical simulation has been performed with $n = 512$, $\mathrm{d}x = 0.25$, $N^0 = 20.48$ and $H^0 = -5.46$.

Before this stationary regime is attained, one can ask how the system finds its road to statistical equilibrium starting from given initial conditions (taken here as homogenous states perturbed by a slight random noise). Since the dynamics after the coalescence regime is quasistatic, converging slowly towards the statistical equilibrium, one can follow this evolution using the average of the particle number spectral density at time t. Here the mean value is taken over the ensemble of 16 initial conditions and also by time averaging over few time units only. Thus the average smoothes the fast variations while the evolutions due to the quasistatic dynamics can be neglected. Fig. 4 shows the particle spectrum for such an intermediate time t_i. The statistical equilibrium has not been reached yet, but the solution has already converged into a single solitary wave surrounded by fluctuations. The spectrum at long wavelengths accounts again for the soliton-like coherent structure containing already

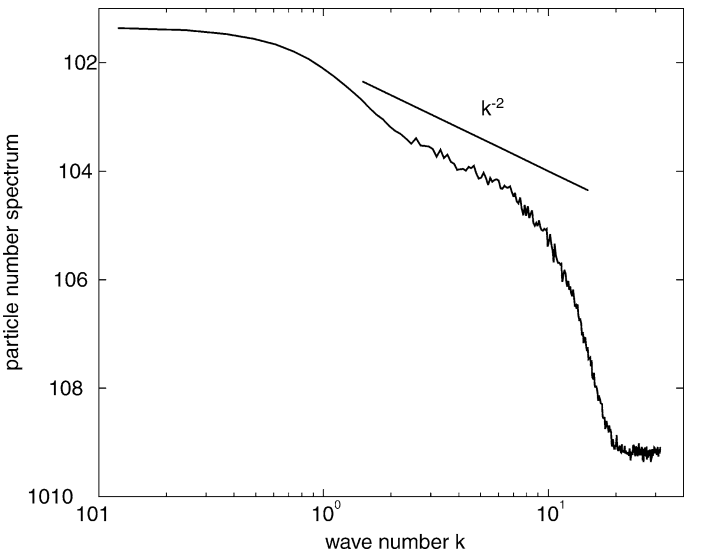

Fig. 4. The particle number spectral density for $n = 512$ and $\mathrm{d}x = 0.1$ (thus $L = 51.2$) at unit time $t = 5 \times 10^5$. The coherent soliton structure already accounts for almost the entire number of particles of the system, but the system has not yet reached statistical equilibrium. The initial noise level is still present for large wavenumbers ($k \geqslant 20$), while at smaller wavenumbers, one can recognize both the soliton-like structure and a fluctuation spectrum following approximately a k^{-2} law. The spectrum has been obtained by an ensemble average over 16 initial conditions and a time average over the final 10 unit times.

almost all the total particles. On the other hand at small scales, the fluctuation modes already exhibit the $1/k^2$ law but only for wavenumbers smaller than a well defined wavenumber $K(t_i)$. For higher wavenumbers, the amplitudes of the fluctuation modes are at the level of the initial noise. Somehow, the system acts as if at each time t the statistical equilibrium (22) were satisfied only for scales larger than $\lambda(t) = 2\pi/K(t)$. As time goes on, the front $k = K(t)$ advances in the momentum space as the 'quasistatic' equilibrium invades smaller and smaller lengthscales. For a finite number of modes, this slow dynamics saturates when all available modes are reached by the equilibrium. Thermal equilibrium between the fluctuations has been attained. The front dynamics is found to obey the scaling $K(t) \simeq t^{1/4}$ using high derivative moments of the wavefunction ψ. It is then tempting to generalize these results to the continuum limit $n \to \infty$. In that case, we expect that at any time the dynamics is made of a solitary coherent structure containing most of the particle number in quasi-statistical equilibrium with a finite number of fluctuating modes. As time goes on, the number of modes at equilibrium increases and the effective temperature due to the equipartition of the energy among the modes decreases. Thus the contribution of the fluctuations to the total mass decreases providing an inverse transfer of mass from the fluctuations to the soliton-like structure. The $t \to \infty$ limit corresponds to *the* coherent structure containing *all* the mass of the system while the excess energy is distributed over an infinite number of modes of zero amplitude!

One may have argued that the prediction of the equipartition of the energy among the modes surrounding a *condensate* structure was obvious since some sort of thermal equilibrium was assumed. In fact, it is noteworthy to observe that the dynamics of (1) reaches in fact a self-thermalized state through the dependence of the temperature with the number n of available modes. The singular limit $n \to \infty$ can then be interpreted as a semi-classical example of the Rayleigh–Jeans paradox [12].

3. Wave turbulence in BEC

We outline here the conclusions of the previous section for a model of BEC. For sake of simplicity and to allow long numerical simulations we will again restrict our study to one spatial dimension. In dimensionless units, the dynamics of a BEC trapped in a harmonic potential can be written [18]:

$$\mathrm{i}\partial_t \psi = \left(-\frac{1}{2}\Delta + V_{\mathrm{ext}}(x) + |\psi|^2\right)\psi, \tag{23}$$

where the additional harmonic potential $V_{\mathrm{ext}}(x) = \frac{1}{2}\Omega^2 x^2$ describes the external potential used to confine the particles in an atomic trap. The usual defocusing nonlinearity corresponding to repulsive particle interactions is used. The integrability of the

1D NLS equation is broken here due to the presence of the external potential V_{ext}. The structure of the equation is clearly equivalent to the general NLS system. The number of particles:

$$N = \int |\psi|^2 \, \mathrm{d}x$$

is conserved as well as the Hamiltonian

$$H = \frac{1}{2} \int \left(|\nabla \psi|^2 + \Omega^2 x^2 |\psi|^2 + |\psi|^4 \right) \mathrm{d}x. \tag{24}$$

To the kinetic energy $|\nabla\psi|^2$ and the nonlinear potential term $|\psi|^4$ is added the contribution of the external potential $\Omega^2 x^2 |\psi|^2$. The solitary solutions $\phi(x)\,\mathrm{e}^{-\imath\mu t}$ which minimize the Hamiltonian for a given number of particles N are solutions of:

$$\mu\phi = -\frac{1}{2}\phi_{xx} + \frac{1}{2}\Omega^2 x^2 \phi + \phi^3 = 0. \tag{25}$$

Such solutions can be obtained numerically and are well described for large enough N by the so-called Thomas–Fermi approximation. Neglecting the kinetic term the Thomas–Fermi solution ϕ_{TF} only balances the nonlinearity and the external potential:

$$\phi_{\text{TF}}(x) = \sqrt{\mu - \frac{1}{2}\Omega^2 x^2}$$

for $|x| \leqslant \sqrt{2\mu}/\Omega$ and $\phi_{\text{TF}}(x) = 0$ elsewhere. By a straightforward integration the chemical potential μ_{TF} satisfies:

$$\mu_{\text{TF}} = \frac{1}{2}\left(\frac{3N\Omega}{2}\right)^{2/3},$$

where N is the total particle number. The radius R_{TF} of the condensate in the Thomas–Fermi approximation is found: $R_{\text{TF}} = (3N/(2\Omega^2))^{1/3}$. Fig. 5 shows solitary solutions of Eq. (25) for different values of N together with the corresponding Thomas–Fermi solution. We observe that the Thomas–Fermi approximation is very good except in a small boundary layer near $x = R_{\text{TF}}$. The potential μ is also found numerically very close to μ_{TF}. The solutions were calculated on the periodic box $x \in [-64, 64]$ of length $L = 128$ unit length, with $\Omega = 0.1$, that we will keep constant throughout, later on.

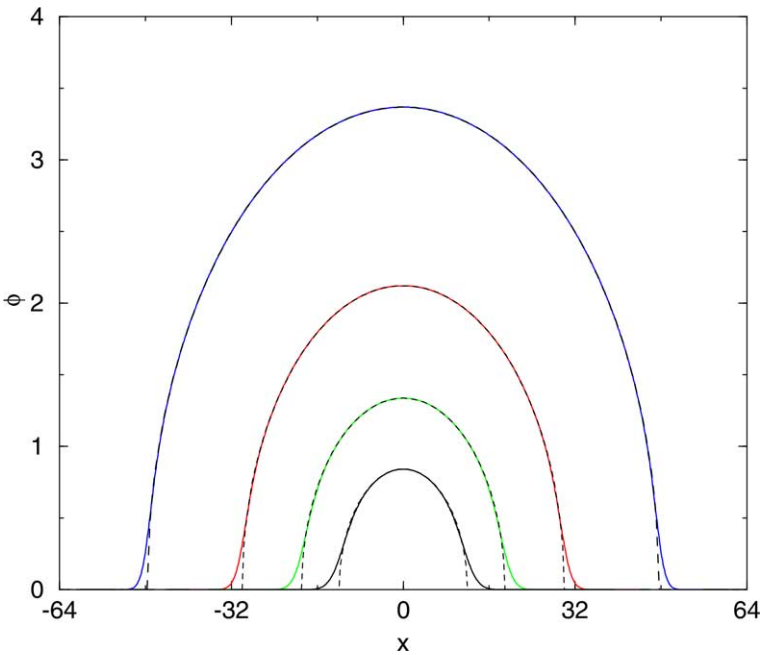

Fig. 5. Solutions $\phi(x)$ of Eq. (25) for $\Omega = 0.1$ and different particle numbers $N = 11.5$, 45, 180 and 720 (as expected, the smaller N the smaller ϕ in the figure). For each solution the dashed line show the Thomas–Fermi approximation ϕ_{TF}.

Perturbations around this ground state are studied to determine the eigenfrequencies of the fluctuation modes. Following Bogoliubov approach, we are seeking solutions for the weak perturbation regime:

$$\psi(x,t) = \left(\phi(x) + u(x)\,\mathrm{e}^{-\mathrm{i}\omega t} + v(x)\,\mathrm{e}^{\mathrm{i}\omega t}\right)\mathrm{e}^{-\mathrm{i}\mu t}.$$

At first order in the complex functions u and v, we obtain from (23) the coupled equations:

$$\omega u(x) = \left(-\frac{1}{2}\partial_{xx} + \frac{1}{2}\Omega^2 x^2 - \mu + 2\phi(x)^2\right)u(x) + \phi(x)^2 v(x), \tag{26}$$

$$-\omega v(x) = \left(-\frac{1}{2}\partial_{xx} + \frac{1}{2}\Omega^2 x^2 - \mu + 2\phi(x)^2\right)v(x) + \phi(x)^2 u(x). \tag{27}$$

This linear system can be solved numerically to determine the excitation spectrum [25]. However, as for the NLS system described above, high frequency modes are well approximated by plane waves $u(x)$, $v(x) \propto \mathrm{e}^{\mathrm{i}kx}$ for small wavelengths such that $k^2 \gg \mu \simeq \mu_{\mathrm{TF}}$. We retrieve then the well-known Bogoliubov relation for high wavenumber dispersive waves

$$\omega = \frac{1}{2}k^2.$$

A priori, the statistical approach developed above applies to this specific NLS system (23). Thus, starting from any initial condition, we should observe the formation of a coherent structure solution of (25) containing almost all the particle number of the system, in the midst of wave fluctuations. For large enough time, one should observe also the statistical equipartition of

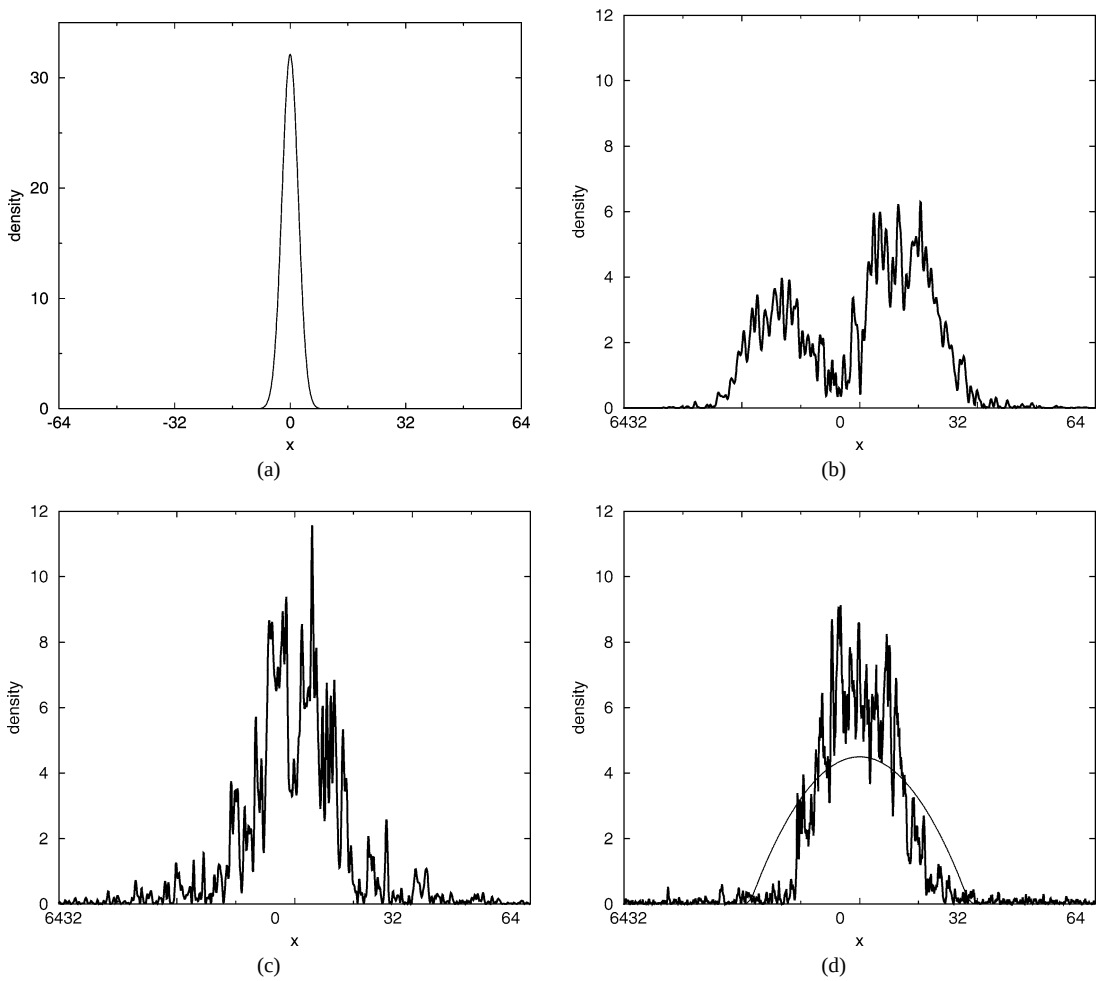

Fig. 6. Particle number density $|\psi(x,t)|^2$ for different times: (a) initial Gaussian profile at $t = 0$, (b) $t = 4000$, (c) $t = 34\,000$ and (d) $t = 250\,000$ units time. The coherent structures containing all the particles is shown as dashed lines on figure (d).

the excess energy between all the available modes for a finite-n grid point calculation. In particular, we should observe again a $1/k^2$ particle number spectrum for large wavenumbers. To illustrate this dynamics, we initiate the dynamics with the ground state of a condensate of noninteracting bosons for $N = 180$. When the nonlinear term is neglected, the ground state of the linear Schrödinger equation is described by a Gaussian distribution of the particle around the trap center:

$$\psi_i(x,t) = \sqrt{N}\left(\frac{\Omega}{\pi}\right)^{\frac{1}{4}} \mathrm{e}^{-(\Omega x^2)/2}\,\mathrm{e}^{-\imath\mu t}.$$

The Gaussian width $\sigma = 1/\sqrt{\Omega}$ defining the typical radius of the noninteracting gas. Numerical simulations are typically made on a regular grid of 512 or 1024 points, using a Yoshida pseudospectral splitting scheme [27] which is 4th order in time. Mass and energy are conserved to within 10^{-10} and 10^{-5} relative errors respectively. At $t = 0$ we start the dynamics of Eq. (23) with:

$$\psi(x,0) = \psi_i(x,0) + \eta(x),$$

where $\eta(x)$ is a white noise of very small amplitude (10^{-5}), taken to break the $x \to -x$ symetry of the system. Fig. 6 shows snapshots of the solution for different times.

We observe roughly the expected dynamics where the coherent structure emerges from fluctuations. However, one can notice that the fluctuation amplitudes are much higher here than for the simulations shown in the previous section, so that the comparison between the solution at large times and the coherent structure (Fig. 6(d)) is only partially satisfied. This high level of fluctuations is due to the large difference of energy between the initial condition ($H = 564.25$) and the coherent structure $\phi(x)$ minimizing the Hamiltonian ($H^* = 486.15$). Moreover, since the initial Gaussian width ($\sigma = 3.16$) is smaller than the Thomas–Fermi radius ($R_{\mathrm{TF}} = 30$) of the coherent structure, we observe in the numerics numerous large radius oscillations around R_{TF} before the solution stabilizes. Such radius oscilations can be noticed between Figs. 6(a–c).

These oscillations and their 'effective' damping are even better seen on Fig. 7 where the different (kinetic, external potential and nonlinear) contributions to the total energy are shown after a short time. Recall that the sum of these three contributions is constant throughout the dynamics. The amplitude of these oscillations are rapidly decreasing after few thousand time units. Thereafter, only small oscillations are observed around slowly varying energy contributions. This slow dynamics is shown in Fig. 8 where again kinetic (bottom curve), and the sum of the external and the potential energies (top curve) are drawn on a much larger time scale. After the short transient, where fluctuations are important, we observe a quasistatic dynamics consisting

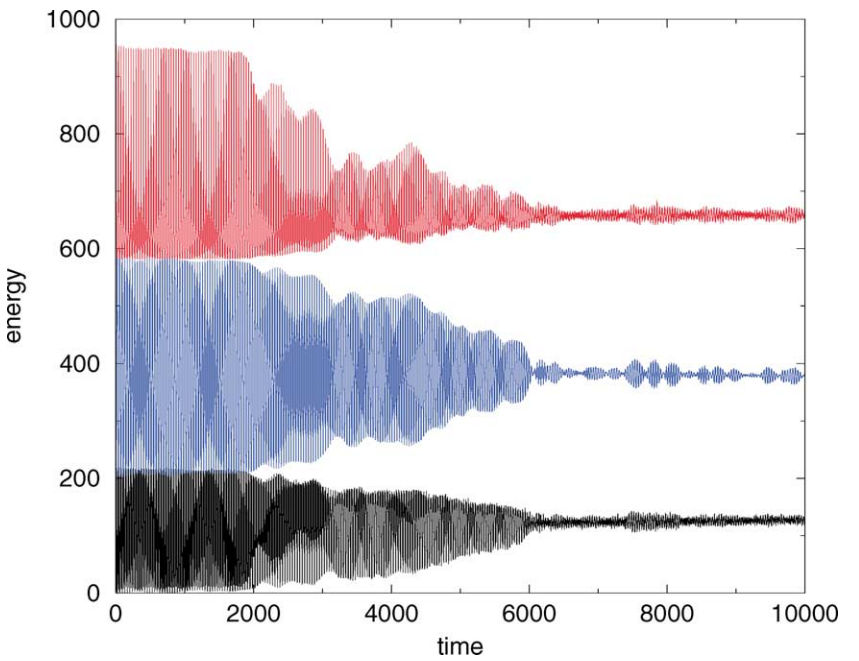

Fig. 7. Different contributions to the total constant energy as functions of time for short times. Kinetic energy (black curve), external potential contribution (red curve) and nonlinear one (blue curve) have been also vertically translated for vizualisation. The calculation is made with $n = 512$ discretization points.

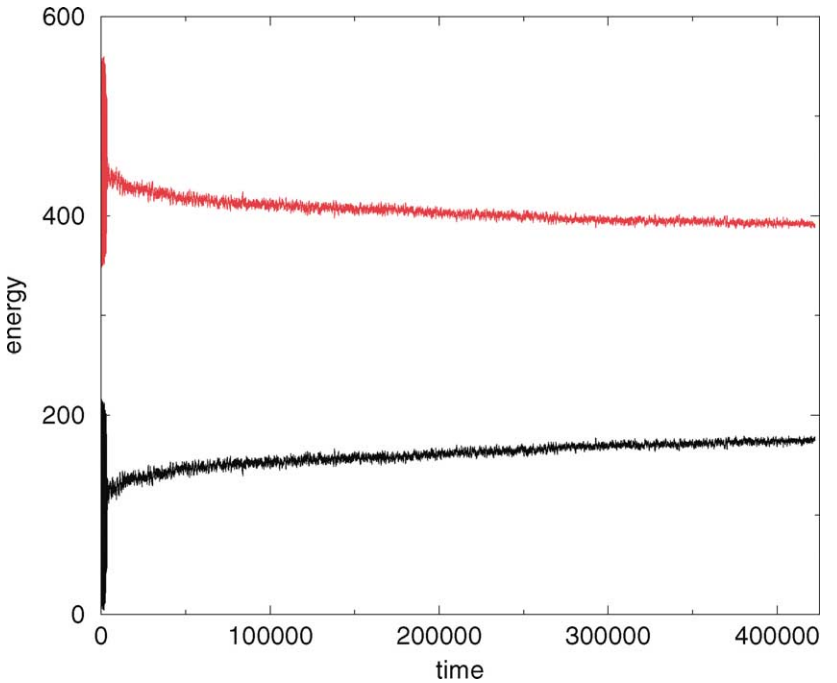

Fig. 8. Kinetic energy (bottom black curve), sum of the external potential and of the nonlinear contribution (top red curve) as function of time. The calculations are made here with $n = 1024$ discretization points.

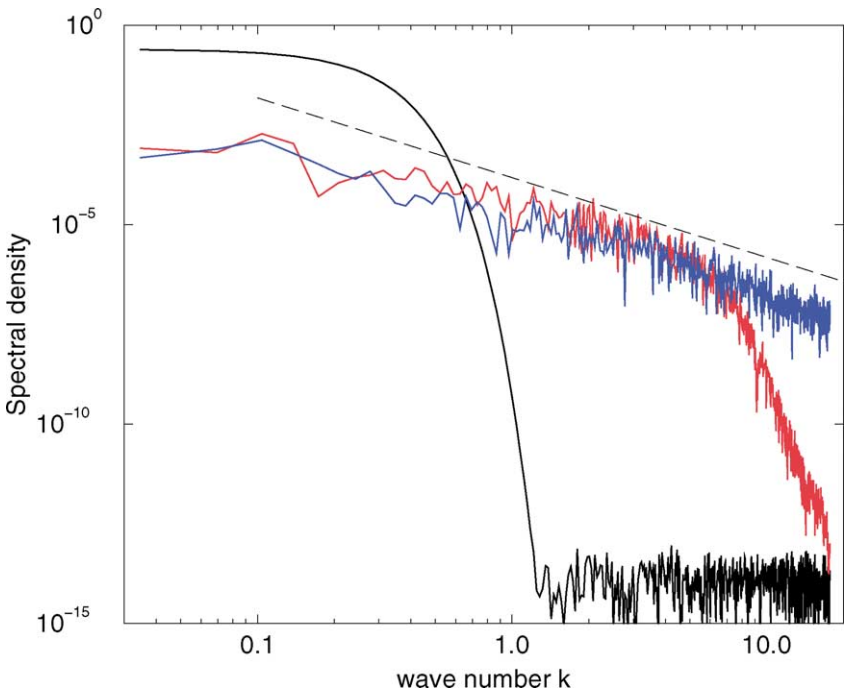

Fig. 9. Particle number spectral density of the fluctuations around the solution $\phi(x)\,\mathrm{e}^{-\mathrm{i}\mu t}$ at different stage of the dynamics on a log–log scale. From bottom to top at high wave number, we have the spectrum of the initial condition $t = 0$ (black curve), the spectrum at $t = 16\,900$ time units (red curve) and at $t = 422\,000$ (blue curve). The dashed line represents the spectral density for large wavenumber as predicted by our theory. The number of grid points for calculation is $n = 1024$ here.

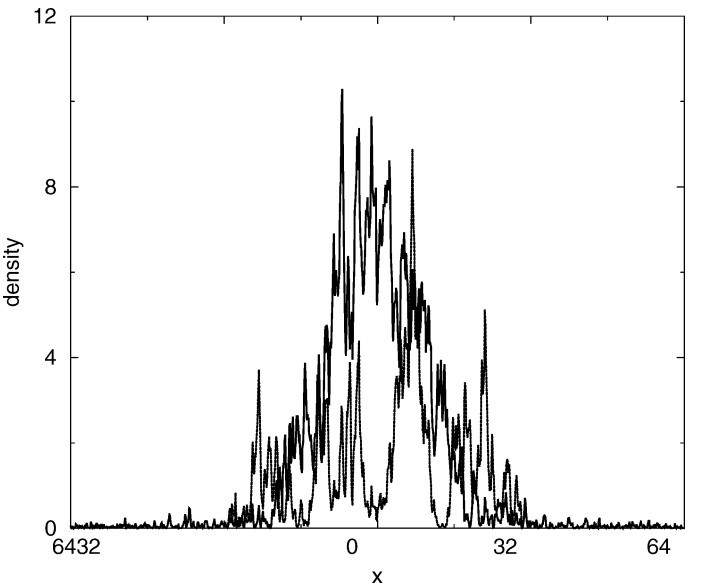

Fig. 10. Particle density $|\psi(x,t)|^2$ (solid line) of the solution of the dynamics (23) and the density of the fluctuation field (dashed curve) at $t = 422\,000$.

of small rapid fluctuations around a slow variation of the energy contribution. As expected, the kinetic contribution increases, while obviously the other contributions decrease. This slow dynamics indicates as for the previous focusing NLS system the transfer of energy towards smaller and smaller scales as time goes on.

The cascade-like transfer can also be seen on Fig. 9 where the particle number spectral density of the fluctuations are shown at different instants of the dynamics. This spectral density is obtained by substracting the coherent structure $\phi\,\mathrm{e}^{-\mathrm{i}\mu t}$ from the solution $\psi(x,t)$. The spectra are obtained by time averaging over one unit of time, except for the initial condition spectrum. One can see the evolution of the spectrum from the initial Gaussian distribution to the predicted spectrum at $t = 422\,000$. The dashed line represents the quantitative prediction $\langle|\psi_j|^2\rangle = (H^0 - H_n^*)/(nk_j^2)$, based on H_n^* calculated with the soliton-like solution containing all the particles ($N = 180$). Such a stationary spectrum corresponding to the statistical equilibrium distribution was actually mostly attained since $t = 200\,000$ time units. The curve at $t = 16\,900$ indicates that the $1/k^2$ spectrum is fist reached at long wavelengths and invades smaller and smaller lengthscales as time goes on, as already observed for the focusing NLS of the previous section.

A difference between the predicted spectrum amplitude at high wave numbers and the numerical results is observed, while the agreement for the focusing NLS in the previous section was much better. We understand such discrepancy by a higher level of fluctuations in the BEC system. The energy difference between the initial condition and the ground state coherent structure containing all the particles is $\Delta H = 78$ here while it was only a few units for the focusing NLS case. Thus the amplitude of the fluctuations are the same order as the coherent structure, as observed in Fig. 10 where, both the density of the numerical simulations and the density of the fluctuation field deduced after subtraction of the expected coherent structures are shown at $t = 422\,000$. Here we are close to the limitation of our approach since the particle number of the fluctuations field is close to the total particle number as discussed previously.

This finite mode self-thermalization of the NLS-like equations has been used recently to model finite temperature BEC [28–30]. Distributing fluctuation energy equally among the Bogoliubov modes, the authors 'mimic' numerically a thermal system at equilibrium with only the Gross–Pitaevskii equation. Although the cutoff at high wavenumbers of the black-body-like catastrophe is needed, we want to emphasize here that this approach is inconsistent since no convergence of this regularization in the continuum limit is proposed. A consistent regularization would have to integrate a quantum description of the dynamics. Our work here, without solving this crucial question, can be seen as an attempt to describe the dynamics of a classical field.

4. Conclusion

We have presented here the asymptotic dynamics of different nonlinear differential equations used to model superfluids and BEC. The description of the statistical properties of the solution for large times when a quasi-static regime is reached has been developped for a finite number of modes truncation. Seeking a stationary probability density function we were led to consider

the maximum entropy density where all the mass is contained in the coherent structure minimizing the Hamiltonian in the continuum limit. Thus, the large scale solutions of the dynamics for a finite number of modes are found by this approach to behave like this coherent structure immerged in a sea of energy equipartitioned fluctuations. Long-time numerical simulations show then very good agreement with the predictions both for a weakly focusing NLS equation and for a 1D version of the BEC model. The road towards these statistically stationary states gives a consistent scenario of the continuum limit of the dynamics. It corresponds to a quasistatic dynamics where the number of fluctuation modes at equilibrium increase with time. The kinetics of the advance towards smaller and smaller scales has been studied for a particular case of NLS dynamics and remains to be fully explored in general.

Acknowledgements

It is my pleasure to thank Richard Jordan with whom this work was initiated. I want also to acknowledge the editors of this special issue for encouraging me to come back to this exciting subject.

References

[1] O. Cardoso, D. Marteau, P. Tabeling, Phys. Rev. E 49 (1994) 454;
J. Paret, P. Tabeling, Phys. Fluids 10 (1998) 3126.
[2] J.C. McWilliams, J. Fluid Mech. 146 (1984) 21;
D. Montgomery, W. Matthaeus, W. Stribling, D. Martinez, S. Oughton, Phys. Fluids A 4 (1992) 3.
[3] A. Hasegawa, Y. Kodama, Solitons in Optical Communications, Oxford University Press, New York, 1995.
[4] B. Rumpf, A.C. Newell, Phys. Rev. Lett. 87 (2001) 54102;
B. Rumpf, A.C. Newell, Physica D 184 (2003) 162–191.
[5] M. Rivera, P. Vorobieff, R. Ecke, Phys. Rev. Lett. 81 (1998) 1417.
[6] H.L. Pesceli, IEEE Trans. Plasma Sci. 13 (1985) 53.
[7] A. Hasegawa, Adv. Phys. 34 (1985) 1.
[8] K.B. Davis, M.-O. Mewes, M.R. Andrews, N.J. van Druten, D.S. Durfee, D.M. Kurn, W. Ketterle, Phys. Rev. Lett. 75 (1995) 3969.
[9] M.H. Anderson, J.R. Ensher, M.R. Matthews, C.E. Wieman, E.A. Cornell, Science 269 (1995) 198.
[10] C.C. Bradley, C.A. Sackett, R.G. Hulet, Phys. Rev. Lett. 75 (1995) 3969.
[11] V.E. Zakharov, A.N. Pushkarev, V.F. Shvets, V.V. Yan'kov, JETP Lett. 48 (1988) 83;
S. Dyachenko, V.E. Zakharov, A.N. Pushkarev, V.F. Shvets, V.V. Yan'kov, Sov. Phys. JETP 69 (1989) 1144.
[12] Y. Pomeau, Nonlinearity 5 (1992) 707;
Y. Pomeau, Physica D 61 (1992) 227.
[13] R. Jordan, C. Josserand, Phys. Rev. E 61 (2000) 1527–1539.
[14] R. Jordan, C. Josserand, Math. Comp. Simulation 55 (2001) 433–447.
[15] R. Jordan, B. Turkington, C.L. Zirbel, Physica D, in press;
Preprint available at http://xxx.lanl.gov/ps/chao-dyn/9904030.
[16] M. Ablowitz, H. Segur, J. Fluid Mech. 92 (1979) 691.
[17] L.P. Pitaevskiĭ, Sov. Phys. JETP 13 (1961) 451;
E.P. Gross, J. Math. Phys. 4 (1963) 195.
[18] F. Dalfovo, S. Giorgini, L. Pitaevskiĭ, S. Stringari, Rev. Mod. Phys. 71 (1999) 463.
[19] J. Bourgain, Commun. Math. Phys. 166 (1994) 1.
[20] V.E. Zakharov, A.B. Shabat, Sov. Phys. JETP 34 (1972) 62;
Y. Li, D. McLaughlin, Commun. Math. Phys. 162 (1994) 175.
[21] P.E. Zhidkov, Soviet Math. Dokl. 43 (1991) 431.
[22] R. Balescu, Equilibrium and Nonequilibrium Statistical Mechanics, Wiley, New York, 1975.
[23] R.S. Ellis, R. Jordan, P. Otto, B. Turkington, Commun. Math. Phys. 244 (2004) 187–208.
[24] J.L. Lebowitz, H.A. Rose, E.R. Speer, J. Statist. Phys. 50 (1988) 657.
[25] M. Edwards, P.A. Ruprecht, K. Burnett, R.J. Dodd, C.W. Clark, Phys. Rev. Lett. 77 (1996) 1671.
[26] A. Picozzi, private communication.
[27] M. Schatzman, private communication.
[28] M.J. Davis, S.A. Morgan, K. Burnett, Phys. Rev. A 66 (2002) 053618.
[29] M.J. Davis, S.A. Morgan, Phys. Rev. A 68 (2003) 053615.
[30] C. Lobo, A. Sinatra, Y. Castin, cond-mat/0301628.